

A Geometric Approach to Designing a Programmable Force Field with a Unique Stable Equilibrium for Parts in the Plane

Attawith Sudsang and Lydia Kavraki
Department of Computer Science
Rice University, Houston, TX 77005, USA
email: {asudsang, kavraki}@cs.rice.edu

Abstract: *In automated assembly, before parts can be put together, they often have to be appropriately oriented and positioned. The device performing this task is generally referred to as a part feeder. A new class of devices for non-prehensible distributed manipulation, such as MEMS actuator arrays, vibrating plates, etc., provides an alternative to traditional mechanical platforms for part feeding. These devices can be abstracted as programmable vector fields. Manipulation plans for these devices can therefore be considered as strategies for applying a sequence of fields to bring parts to some desired configurations. Typically, to uniquely orient and position a part, several fields have to be sequentially employed. In this paper, we show that this objective can be achieved for most parts using a single field. The key idea is that, for almost any part (1) there exists a single field that induces a unique stable equilibrium for the part, and (2) when the part is placed under the field, it is essentially driven toward the associated stable equilibrium configuration.*

It has been proven recently that there exists a combination of the unit radial field and a constant field that induces a unique stable equilibrium for almost any part. However, the work focuses mainly on an existential proof and fails to address how to compute the field for a given part. We propose in this paper a radically different field with a proof confirming that the field induces a unique stable equilibrium for almost any part. This proof leads us to a method for computing a single field for orienting a given part, together with the corresponding stable equilibrium configuration of the part.

1 Introduction

In automated assembly, before parts can be put together, they often have to be appropriately oriented and positioned. The device performing this task is generally referred to as a part feeder. The traditional and mostly used automated part feeder is the vibratory bowl feeder [8]. Vibratory bowl feeders are designed to orient a single part shape, therefore they have to be re-designed and re-built to

handle different shapes. Some recent research attempts to develop systematic approaches for designing and analyzing vibratory bowl feeders [2, 13], while the mainstream research in manufacturing has focused in developing more flexible and more robust platforms, such as programmable part feeders. This type of part feeder can be programmed to handle different parts without the need for hardware modification [9, 12, 10, 1, 7].

A new direction in programmable part feeding that has recently gained attention in research is the use of a new class of devices for non-prehensible distributed manipulation. Examples are, in microscale, the use of MEMS actuator arrays [4], and in macroscale, the use of mechanical devices [16], vibrating plates [7], or air jets actuators [3]. The analysis of the capabilities of these devices is based on the abstraction of these devices as programmable vector fields. This analytical approach is pioneered by [4], where programmable vector fields are used to represent MEMS actuator array, and the properties of some certain force fields have been discussed. The underlying idea is that a part lying in a force field is driven toward a stable equilibrium by the resultant force and torque induced by the field at the planar contact. This basic idea allows a manipulation task to be considered as a strategy for applying a sequence of fields to bring a part from one equilibrium to another until it reaches a desired configuration. In [4], it has been shown that polygonal parts can be oriented by a sequence of squeeze fields. The sequence is planned using an algorithm similar to the one in [12] for orienting polygonal parts with a sensorless parallel jaw gripper. The number of steps in the sequence depends on the complexity of the geometry of the convex hull of the oriented part and the uniqueness of the final orientation is only upto modulo 180° . Another research direction attempting to apply force fields to the positioning problem aims at inventing a single force field that can induce a unique stable equilibrium for any part. Such a field would be able to orient any part in one step without any sensor or any sequencing control. Along this avenue, the elliptical force field that induces two stable equilibria was introduced in [14]. Further progress was presented recently in [6] with a proof

confirming the conjecture in [4], namely, that there exists a combination of the unit radial field and a small constant field capable of uniquely orienting and positioning parts. The proof is based on characterization of local minima of the lifted potential function induced by the field. Unfortunately, due to the nature of the proof, this work cannot address how to compute a finite magnitude of the small constant field that satisfies the proof. Therefore it is impossible to explicitly specify the field for a given part. Instead, the determination of the value of the constant field value is done experimentally using a standard search procedure.

In this paper, we will introduce a force field that induces a unique stable equilibrium for almost any part with uniform support. This proposed field is a combination of a linear radial force field and a constant force field. A linear radial force field is simply a radial force field for which the magnitude of the force at a point is a linear function of the distance from the point to the center of the field. The proposed field is therefore defined by the parameters consisting of the magnitude of the constant force field and the coefficients defining the linear function associated with the linear radial force field. The main goal of this paper is to prove that, for a given part, we can specify the parameters of the proposed field such that the part has a unique stable equilibrium when it is placed under this parameterized field. The proof relies on geometric relationship between the proposed field and the inducing force and torque. This relationship will be presented in Section 4 and the main proof will be presented in Section 5. The proof begins by specifying the parameters of the field according to the geometry of a given part. For this parameterized field, the proof then continues with the following two steps. The first step applies some geometric properties of constant fields and linear radial fields, which will be presented in Section 4, to show that there are at most two possible equilibrium configurations. Then, based on the potential function concept which will be discussed in Section 3, the second step determines that only one of the two equilibria is stable. Unlike [6], the values of all parameters of the field for orienting a given part can be determined. The determination requires the computation of a unique point of the part which we will call a pivot point. This computation is presented in [19].

The rest of the paper is organized as follows. We will begin by giving some background and necessary notations in Section 2. Then, the concept of potential function which will be used for determining stability will be presented in Section 3. In Section 4, some properties of constant fields and linear radial force fields which are the foundation of the proof of the main result will be presented. Then, in Section 5, we will present Lemma 5 which constitutes the main result describing the proposed

field with a proof verifying that it induces a unique stable equilibrium for almost any given part. Throughout this paper, when we mention the main result, we refer to Lemma 5 and likewise when we mention the main proof, we refer to the proof of Lemma 5. We will then conclude the paper with some discussion in Section 6.

2 Background

We consider a two dimensional part with a uniform mass and area A that is placed in the plane of a force field. We attach the world frame (ξ, η) to this plane.

The part is in equilibrium under the field $\mathbf{g}(\xi, \eta)$ when the resultant force \mathbf{F} and torque \mathbf{M} vanish. More precisely, an *equilibrium* is achieved if and only if

$$\mathbf{F} = \int \int \mathbf{g}(\xi, \eta) d\xi d\eta = 0 \quad \text{and}$$

$$\mathbf{M} = \int \int \begin{pmatrix} \xi \\ \eta \end{pmatrix} \times \mathbf{g}(\xi, \eta) d\xi d\eta = 0,$$

where both integrations are performed over the plane region occupied by the part. Note that the lateral force modeling used here results in first order dynamics of the motion of parts under force fields. It is a commonly used hypothesis in part orientation with force fields [5, 4, 14].

In this paper, we deal with only two types of force fields: constant fields and radial fields. A *constant field* is a force field with the same force at every point and a *radial field* is a force field for which all forces point toward a single center and the magnitude of the force at a point depends only on the distance between the point and the center. It is clear from the definition above that the resultant force induced by a radial field must pass through the center of the field (this simple property will become useful later on). We denote by a tuple $\langle c, f(\lambda) \rangle$ a radial field with center c and the force at any point \mathbf{p} be the unit force in the direction from \mathbf{p} to c , scaled by $f(\lambda)$ where λ is the distance between \mathbf{p} and c . Note that a linear radial field is a radial field for which the function f is linear in λ . We also use a pictorial representation to illustrate a radial field. Figure 1 shows an example.

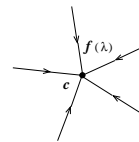


Figure 1: Pictorial representation of the radial field $\langle c, f(\lambda) \rangle$, with $f(\lambda) \geq 0$. The arrows on the rays depict the direction of the forces.

We define the *pivot point*¹ of a part under a radial field

¹ We borrow this term from [4] where it is defined only for the unit radial field.

to be a fixed point in the part's coordinate frame situated at the center of the field when an equilibrium is achieved (see Lemma 4 for the uniqueness of the pivot point under some radial fields).

3 Potential Function

Consider a two dimensional part with a uniform mass that is placed in the plane of a force field. Under this force field, let $u : \mathbb{R}^2 \mapsto \mathbb{R}$ be a potential function of a particle in the plane (ξ, η) . From mechanics [15, 18], the force exerted on the particle under this potential function is $(-\frac{\partial u}{\partial \xi}, -\frac{\partial u}{\partial \eta})^T$. Because a rigid part is essentially a system of particles, its potential energy is thus the summation of the potential energies of all the particles. Given that $\begin{pmatrix} x \\ y \end{pmatrix}$ is the position in the world frame (ξ, η) of a reference point in the part frame and θ is the orientation of the part frame with respect to the world frame, the potential energy of the part at a configuration $\mathbf{q} = (x, y, \theta)$ can be written as

$$U(\mathbf{q}) = \int \int u(\xi, \eta) d\xi d\eta,$$

where the integration is performed over the plane region occupied by the part at the configuration \mathbf{q} . To distinguish from the potential function of a particle, we call $U : \mathbb{R}^2 \times S^1 \mapsto \mathbb{R}$ the lifted potential function (after [6]). It can be shown [6] (using continuity of u and the compactness of the part) that U is a continuous function of class \mathcal{C}^1 and (using commutativity of the integral and differential operators) that the wrench $(F_x, F_y, M)^T$ exerted on the part can be written as:

$$\begin{aligned} F_x(\mathbf{q}) &= -\partial U / \partial x, \\ F_y(\mathbf{q}) &= -\partial U / \partial y \text{ and} \\ M(\mathbf{q}) &= -\partial U / \partial \theta. \end{aligned} \quad (1)$$

In other words, we may consider the part as a particle rolling on the hyper-surface U under the influence of the force derived from the surface's negative gradient. Clearly, when this particle is at a critical point of the surface, the surface's gradient becomes zero and as a result the part is in an equilibrium because the force vanishes. From the type of the associated critical point (i.e., local minima, local maxima, saddle points [17]), we can also determine the stability of the equilibrium. It is well known that only local minima correspond to stable equilibrium configurations.

It is important to keep in mind that every smooth force field has an associated potential function counterpart. This allows us to apply the concept mentioned above to investigate the stability of an equilibrium configuration in the second step of the main proof.

4 Geometry of Force Fields

As mentioned earlier, the proposed force field is a combination of a linear radial field and a constant field. This section studies some properties of these two types of fields that are helpful for deriving the main proof. Instead of purely analyzing the fields algebraically, we seek geometric explanations. As we will see soon, this approach nicely yields intuitive insight about the fields.

We will begin with the following lemma which is a crucial part of the work in this paper. It demonstrates how to decompose a constant field into two radial fields. Its significance is that the resulting two radial fields can be freely translated and the distance between their centers can be varied. This freedom allows geometric manipulation of the fields as we can choose to place the two fields in such a way that our analysis can be simplified. This benefit will become clearer in the next section where this strategy is thoroughly used.

Lemma 1 *The constant field $\begin{pmatrix} -\delta \\ 0 \end{pmatrix}$ is equivalent to the combination of two radial fields $\mathcal{J}_1 \stackrel{\text{def}}{=} \langle \begin{pmatrix} e \\ f \end{pmatrix}, k\lambda \rangle$ and $\mathcal{J}_2 \stackrel{\text{def}}{=} \langle \begin{pmatrix} e+d \\ f \end{pmatrix}, -k\lambda \rangle$, where $kd = \delta$ (Figure 2).*

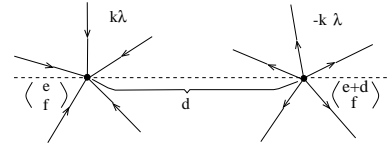


Figure 2: Decomposing a constant field into two radial fields.

PROOF: Clearly, at an arbitrary point $\begin{pmatrix} s \\ t \end{pmatrix}$, the force induced by \mathcal{J}_1 is $k \begin{pmatrix} e-s \\ f-t \end{pmatrix}$ and the force induced by \mathcal{J}_2 is $-k \begin{pmatrix} e+d-s \\ f-t \end{pmatrix}$ (see Figure 3). Thus, the resultant force from both fields at the point $\begin{pmatrix} s \\ t \end{pmatrix}$ is given by $k \begin{pmatrix} e-s-e-d+s \\ f-t-f+t \end{pmatrix} = -k \begin{pmatrix} d \\ 0 \end{pmatrix}$. ■

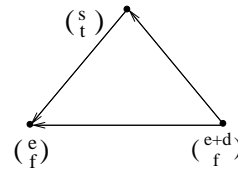


Figure 3: An arbitrary point $\begin{pmatrix} s \\ t \end{pmatrix}$ with respect to the two radial fields' centers.

The following two lemmas express the relationship between the resultant forces induced by the fields and the vectors from the pivot points to the centers of the fields. This geometric relationship is very helpful as we can use it to visualize the effect of the fields on a part at different configurations. In the main result, these two lemmas provide important constraints for identifying possible locations of two pivot points at an equilibrium configuration.

Lemma 2 For the resultant force \mathbf{F} induced by the radial field $\mathcal{J} \stackrel{\text{def}}{=} \langle \mathbf{o}, h + k\lambda \rangle$ on a part, it is true that $\mathbf{F} \cdot \overrightarrow{\mathbf{p}\mathbf{o}} \geq 0$ and $|\mathbf{F}| \geq k|\mathbf{p}\mathbf{o}|A$, where constants $h, k > 0$ and \mathbf{p} denote the position of the pivot point of the part under the field \mathcal{J} (Figure 4).

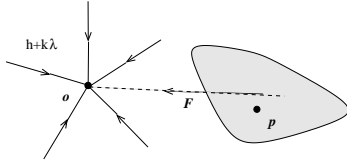


Figure 4: The resultant force \mathbf{F} induced by the radial field $\langle \mathbf{o}, h + k\lambda \rangle$.

The proof of this lemma can be found in Appendix of the paper.

Lemma 3 The resultant force induced by the radial field $\langle \mathbf{o}, k\lambda \rangle$ on a part is $k\overrightarrow{\mathbf{p}\mathbf{o}}A$, where \mathbf{p} denotes the position of the centroid of the part (Figure 5).

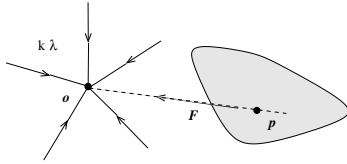


Figure 5: The resultant force \mathbf{F} induced by the radial field $\langle \mathbf{o}, k\lambda \rangle$.

The proof of this lemma is similar to that of Lemma 2 and is omitted here. The key idea is that the pivot point under the field $\langle \mathbf{o}, k\lambda \rangle$ is the centroid of the part. This fact follows immediately from the definition of the centroid [18].

Lemma 4 A part under the non-zero radial field $\mathcal{J} \stackrel{\text{def}}{=} \langle \mathbf{o}, h + k\lambda \rangle$, $h, k \geq 0$ has a unique pivot point.

The proof of this lemma can be found in Appendix of the paper. In the main result, this lemma is used together with Lemmas 2 and 3 to identify all possible equilibrium configurations.

5 The Proposed Field

The following lemma presents the main result. In the proof of the lemma, we put together the material we have discussed so far to show that a combination of the radial field \mathcal{J}^* and the constant field \mathcal{C}^* induces a unique stable equilibrium for almost any part. The proof consists of two steps. The objective of the first step is to identify all possible equilibrium configurations. We transform the constant field \mathcal{C}^* into two radial fields (Lemma 1), one of which is placed to coincide and combine with the radial field \mathcal{J}^* . The analysis is then performed on the arrangement of the pivot points under the two resulting radial fields with respect to the centers of the fields. Based mainly on Lemmas 2 and 3, there are two such arrangements possible at equilibrium. In the second step of the proof, using the potential function concept, we show that one of the two arrangements corresponds to an unstable configuration, while the other corresponds to a stable equilibrium configuration.

Lemma 5 Let h, k and c be arbitrary positive constants, and let d be the distance between the centroid and the pivot point of a part under the radial field $\mathcal{K} \stackrel{\text{def}}{=} \langle \mathbf{o}, h + (k + c)\lambda \rangle$. If $d > 0$, then the part has a unique stable equilibrium configuration under the combination of the radial field $\mathcal{J}^* \stackrel{\text{def}}{=} \langle \mathbf{o}, h + (2k + c)\lambda \rangle$ and the constant field $\mathcal{C}^* \stackrel{\text{def}}{=} \begin{pmatrix} -kd \\ 0 \end{pmatrix}$. This stable equilibrium occurs when the part is in the configuration such that its pivot point under \mathcal{K} is positioned at \mathbf{o} and its centroid is positioned at $\mathbf{o} - \begin{pmatrix} d \\ 0 \end{pmatrix}$.

Before proceeding to the proof, note that determining the distance d for a given part requires the computation of the part's centroid and the part's pivot point under the radial field \mathcal{K} . Because the centroid of a part is essentially the center of the distribution of the part's area, it can therefore be computed, in general, using a numerical integration method. The pivot point can be computed using a numerical optimization of the corresponding potential function. We present in detail in [19] a variation of this optimization approach for computing the pivot point under a linear radial field that is of the same type as that of \mathcal{K} .

PROOF:

STEP 1: Identifying Possible Equilibria

Without loss of generality, let us assume that $\mathbf{o} = \begin{pmatrix} 0 \\ 0 \end{pmatrix}$. From Lemma 1, the constant field \mathcal{C}^* is equivalent to the combination of two radial fields $\langle \mathbf{o}' = \begin{pmatrix} -d \\ 0 \end{pmatrix}, k\lambda \rangle$

and $\langle \mathbf{o}, -k\lambda \rangle$. Combining these two radial fields with \mathcal{J}^* yields two radial fields $\mathcal{K}' \stackrel{\text{def}}{=} \langle \mathbf{o}', k\lambda \rangle$ and $\mathcal{K} \stackrel{\text{def}}{=} \langle \mathbf{o}, h + (2k + c)\lambda - k\lambda \rangle = \langle \mathbf{o}, h + (k + c)\lambda \rangle$. Now let us consider the fields \mathcal{K}' and \mathcal{K} and denote respectively by \mathbf{F}' and \mathbf{F} their inducing forces. At an equilibrium, it is necessary that the line of action of the force \mathbf{F}' coincides with the x-axis (otherwise, a non-zero moment will result). For the line of action of the force \mathbf{F}' to coincide with the x-axis, following Lemma 3, the centroid must be on the x-axis.

At an equilibrium configuration, let us denote by $\mathbf{p}' = \begin{pmatrix} e \\ 0 \end{pmatrix}$ the position of the centroid (the pivot point under \mathcal{K}'), and by \mathbf{p} the position of the pivot point under \mathcal{K} . We consider two cases:

- case $e \leq 0$

Since the distance between \mathbf{p} and \mathbf{p}' is defined to be d , we can write $\mathbf{p} = \mathbf{p}' + d \begin{pmatrix} \cos \phi \\ \sin \phi \end{pmatrix} = \begin{pmatrix} e + d \cos \phi \\ d \sin \phi \end{pmatrix}$, where ϕ is the angle between $\overrightarrow{\mathbf{p}'\mathbf{p}}$ and the x-axis. Straightforwardly, we obtain $|\mathbf{p}\mathbf{o}|^2 - |\mathbf{p}'\mathbf{o}'|^2 = 2de(\cos \phi - 1)$, which implies that $|\mathbf{p}\mathbf{o}| \geq |\mathbf{p}'\mathbf{o}'|$ (when $e \leq 0$). From Lemma 3, we can write $|\mathbf{F}'| = k|\mathbf{p}'\mathbf{o}'|A$ and from Lemma 2, we can write $|\mathbf{F}| \geq (k + c)|\mathbf{p}\mathbf{o}|A$. We then obtain

$$|\mathbf{F}| - |\mathbf{F}'| \geq \{k(|\mathbf{p}\mathbf{o}| - |\mathbf{p}'\mathbf{o}'|) + c|\mathbf{p}\mathbf{o}|\}A.$$

Clearly, at an equilibrium, it is necessary that $|\mathbf{F}| - |\mathbf{F}'| = 0$. This condition implies that the right side of the above inequality must be zero. Because $|\mathbf{p}\mathbf{o}| \geq |\mathbf{p}'\mathbf{o}'|$, as established earlier, this can occur only at a configuration for which $|\mathbf{p}\mathbf{o}| = |\mathbf{p}'\mathbf{o}'| = 0$. From the fact that the centroid and the pivot point under \mathcal{K} are unique (Lemma 4), when $d > 0$ (i.e., $\mathbf{p} \neq \mathbf{p}'$), it is obvious that this configuration is unique. In fact, it is an equilibrium configuration because both pivot points are situated at their centers and therefore $\mathbf{F}' = \mathbf{F} = 0$ (Figure 6).

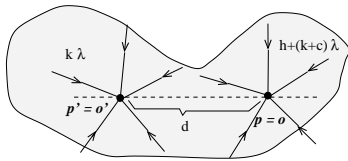


Figure 6: The equilibrium configuration with the two pivot points at the corresponding centers ($\mathbf{p}' = \mathbf{o}'$ and $\mathbf{p} = \mathbf{o}$).

- case $e > 0$

Let us assume that the part is in equilibrium when $e = e' > 0$. From Lemma 1, we can write the constant field \mathcal{C}^*

as a combination of the radial fields $\langle \mathbf{o} = \begin{pmatrix} 0 \\ 0 \end{pmatrix}, \frac{kd}{e'}\lambda \rangle$ and $\langle \mathbf{e}' = \begin{pmatrix} e' \\ 0 \end{pmatrix}, -\frac{kd}{e'}\lambda \rangle$. Combining these two fields

with \mathcal{J}^* yields two radial fields $\mathcal{L} \stackrel{\text{def}}{=} \langle \mathbf{o}, h + (2k + c)\lambda + \frac{kd}{e'}\lambda \rangle$ and $\mathcal{L}' \stackrel{\text{def}}{=} \langle \mathbf{e}', -\frac{kd}{e'}\lambda \rangle$. When the centroid is positioned at \mathbf{e}' , the resultant force induced by \mathcal{L}' is zero. An equilibrium can be achieved only when the resultant force induced by \mathcal{L} is also zero. This occurs when the pivot point under \mathcal{L} is positioned at \mathbf{o} . By Lemma 4, this configuration is unique. That is, we have shown that for a given e' , the associated equilibrium is unique. It is also easy to see that e' is unique as we can reduce the proof of the uniqueness of e' to the proof of the previous case ($e \leq 0$) by replacing \mathcal{K} with \mathcal{L} and \mathcal{K}' with \mathcal{L}' . As a result, we can conclude that if an equilibrium exists in this case, it is unique.

STEP 2: Analyzing Stability

In the previous step, we have shown that there are at most two equilibrium configurations. Here, we will first show that the possible equilibrium found in the case $e > 0$ is unstable. Then we will prove the existence of a local minimum of the lifted potential function of the proposed field (the combination of the field \mathcal{J}^* and the field \mathcal{C}^*). This will deduce that the equilibrium configuration found in the case $e \leq 0$ is the unique stable equilibrium.

Consider the part under the field \mathcal{L}' alone. Let us denote by $U_{\mathcal{L}'}$ the associated lifted potential function. Because \mathcal{L}' is rotational symmetric about the center, it is sufficient to consider the part at a fixed orientation. For convenience, let the centroid be the reference point of the part frame. For the fixed orientation, this setup deduces that the configuration of the part is the position of the centroid and the equilibrium configuration under \mathcal{L}' is the position of the center of the field \mathcal{L}' (because the part is in equilibrium when the position of the centroid is at the center of \mathcal{L}'). From Lemma 3, the resultant force always points in the direction from the center of \mathcal{L}' to the centroid. Following Equation 1, this means that the gradient of $U_{\mathcal{L}'}$ always points toward the equilibrium configuration, and therefore, the lifted potential function $U_{\mathcal{L}'}$ is maximized there.

Now let us consider the part under both fields \mathcal{L} and \mathcal{L}' and denote by U the associated lifted potential function. Let τ be the set of all configurations for which the pivot point under \mathcal{L} is positioned at the center of \mathcal{L} (this set is homeomorphic² to \mathcal{S}^1). Obviously, \mathcal{L} exerts a zero force on the part at any configuration in the set τ . Therefore, the gradient of U at any configuration in the set τ is essentially the gradient of $U_{\mathcal{L}'}$ at the same configuration

²topologically equivalent

and the lifted potential function U on the set τ is simply a copy of the lifted potential function $U_{\mathcal{L}'}$ (with a constant shift). Clearly, the set τ contains the possible equilibrium configuration found in the case $e > 0$. At this configuration, the centroid is positioned at the center of the field \mathcal{L}' , which maximizes the lifted potential function $U_{\mathcal{L}'}$ as established in the previous paragraph. This means that the lifted potential function U of this configuration is greater than that of other configurations in the set τ . Since τ is connected, we can conclude that this configuration is not a local minimum, and therefore is unstable.

We have shown that if there exists an equilibrium according to the case $e > 0$ (existence is not proven), it is unstable. To ensure that the equilibrium according to the case $e \leq 0$ is stable, in the following paragraph, we will prove the existence of a local minimum of the lifted potential function associated with the proposed field.

Let us denote by U the lifted potential function of the proposed field (the combination of the field \mathcal{J}^* and the field \mathcal{C}^*). Straightforwardly, the function U is induced from the potential function $u(\xi, \eta) = kd\xi + h\sqrt{\xi^2 + \eta^2} + \frac{2k+c}{2}(\xi^2 + \eta^2)$, where $\begin{pmatrix} \xi \\ \eta \end{pmatrix}$ is a position in the plane of the proposed field (coordinates of the world frame). When the part is at an arbitrarily fixed orientation θ , it is obvious that as the configuration of the part diverges (in any direction), the potential energy increases toward infinity. Together with the fact that the function U is smooth, this implies that for the given fixed orientation θ , the function U has a local minimum. Let us denote by $U^*(\theta)$ the potential energy of the local minimum at the orientation θ and consider the curve γ of $U^*(\theta)$ for $\theta \in \mathcal{S}^1$. The curve γ corresponds to all the configurations for which the force components F_x and F_y are zero. At a critical point of γ , we also have zero moment because $\partial U / \partial \theta = 0$. This means that a critical point of γ corresponds to an equilibrium configuration. Because the lifted potential function U is smooth, $\theta \in \mathcal{S}^1$ and the number of equilibria is at most two, the curve γ has a local minimum (this also means that γ has a local maxima and in turn implies the existence of the unstable equilibrium). This is clearly also a local minimum of U and completes the proof. ■

Now, let us discuss about the set of parts proven to have a unique stable equilibrium under the proposed field. As mentioned explicitly in Lemma 5, these are the parts having the pivot point under the radial field \mathcal{K} apart from the centroid. Note that they are the same as the set of parts proven to have a unique stable equilibrium in [6] which are the parts whose the centroid does not coincide with the pivot point under the unit radial field (see [11] for some analysis about this case). The equivalence can be shown using Lemma 4). Clearly, most parts assuming arbitrarily general shapes are included in this set. Some particular

classes of parts, however, do not, e.g., parts with at least two axes of symmetry.

6 Conclusion

Although a fully programmable continuous force field device does not currently exist, the research aiming at developing this technology has advanced so rapidly that it would be at no surprise if such a device appeared in the near future. While waiting for an arrival of the new technology, we find it interesting and useful to investigate properties of some force fields. The main contribution of this paper is a force field with a unique stable equilibrium configuration for most parts. The field is proposed to be used for orienting and positioning parts in the plane. The use of force fields as a modeling tool for physical force field devices is a common practice because it usually leads to tractable analytical results. Although this modeling scheme is considered reasonable, it does not capture the discretization nature of a force field implementation and some real-world effects such as friction and surface tension. This limitation exposes the scheme to some legitimate questions, for example: Will the part stop at the computed equilibrium if friction is considered?, What is the convergence rate of a part under the field?, and so on. Without considering a specific implementation and the corresponding dynamics, it is generally impossible to answer these questions. This may lead to future work targeting at filling the gap between available theories and new technologies as they arrive. Our specific research plans include identifying other interesting fields and their properties, and investigating discretized force fields.

Acknowledgements

Work on this paper by Attawith Sudsang and Lydia Kavradi has been supported in part by NSF IRI-970228, NSF CISE SA1728-21122N and a Sloan Fellowship to Lydia Kavradi.

Appendix

Proof of Lemma 2

Without loss of generality, let us assume that $\mathbf{o} = \begin{pmatrix} 0 \\ 0 \end{pmatrix}$, and rewrite the field \mathcal{J} as the combination of two radial fields $\mathcal{J}_1 \stackrel{\text{def}}{=} \langle \mathbf{o}, k\lambda \rangle$ and $\mathcal{J}_2 \stackrel{\text{def}}{=} \langle \mathbf{o}, h \rangle$. Let us denote by $\mathbf{f}_1, \mathbf{f}_2 : \mathbf{R}^2 \mapsto \mathbf{R}^2$ the functions that map point positions in the world frame to the forces at the positions induced by \mathcal{J}_1 and \mathcal{J}_2 correspondingly. Also, let us denote by P the pivot point under \mathcal{J} and by M an arbitrary point of

the part. Let \mathbf{p} and $\mathbf{m} = \begin{pmatrix} \xi \\ \eta \end{pmatrix}$ denote the positions of P and M in the world frame when the part is at a configuration \mathbf{q} .

By setting $\mathbf{g}_i(\mathbf{m}) = \mathbf{f}_i(\mathbf{m}) - \mathbf{f}_i(\mathbf{m} - \mathbf{p})$, for $i = 1, 2$, we can write the resultant force at \mathbf{m} as $\mathbf{f}(\mathbf{m}) = \mathbf{f}_1(\mathbf{m}) + \mathbf{f}_2(\mathbf{m}) = \mathbf{f}_1(\mathbf{m} - \mathbf{p}) + \mathbf{f}_2(\mathbf{m} - \mathbf{p}) + \mathbf{g}_1(\mathbf{m}) + \mathbf{g}_2(\mathbf{m})$ and we can write the resultant force \mathbf{F} exerted on the part at the configuration \mathbf{q} as

$$\begin{aligned} \int \int \mathbf{f}_1(\mathbf{m}) + \mathbf{f}_2(\mathbf{m}) d\xi d\eta = & \int \int \mathbf{f}_1(\mathbf{m} - \mathbf{p}) + \mathbf{f}_2(\mathbf{m} - \mathbf{p}) d\xi d\eta + \\ & \int \int \mathbf{g}_1(\mathbf{m}) d\xi d\eta + \\ & \int \int \mathbf{g}_2(\mathbf{m}) d\xi d\eta, \end{aligned} \quad (2)$$

with all the integrations performed over the plane region occupied by the part at the configuration \mathbf{q} . It is easy to see that the first term of the right side of Equation 2 vanishes. This is because $\mathbf{f}_1(\mathbf{m} - \mathbf{p}) + \mathbf{f}_2(\mathbf{m} - \mathbf{p})$ is essentially the force at the point M when the part is at the configuration such that the pivot point P is positioned at the field's center \mathbf{o} and the orientation of the part is the same as that of the configuration \mathbf{q} . We therefore need to consider only the second and the third terms.

Consider the second term of the right side of Equation 2. From the definition, we have $\mathbf{g}_1(\mathbf{m}) = \mathbf{f}_1(\mathbf{m}) - \mathbf{f}_1(\mathbf{m} - \mathbf{p}) = (-k\mathbf{m}) - (-k(\mathbf{m} - \mathbf{p})) = -k\mathbf{p} = k\overline{\mathbf{p}\mathbf{o}}$. As a result, we obtain $\int \int \mathbf{g}_1(\mathbf{m}) d\xi d\eta = k\overline{\mathbf{p}\mathbf{o}}A$.

Now consider the third term of the right side of Equation 2. Let $a = |\mathbf{p}\mathbf{m}|$, $b = |\mathbf{o}\mathbf{m}|$, $\alpha = \angle \mathbf{p}\mathbf{m}\mathbf{o}$, and ϕ be the angle between $\overline{\mathbf{m}\mathbf{p}}$ and the x-axis (Figure 7). We can write

$$\begin{aligned} \mathbf{f}_2(\mathbf{m}) &= h \begin{pmatrix} \cos(\phi + \alpha) \\ \sin(\phi + \alpha) \end{pmatrix}, \\ \mathbf{f}_2(\mathbf{m} - \mathbf{p}) &= h \begin{pmatrix} \cos \phi \\ \sin \phi \end{pmatrix}, \\ \mathbf{p} &= \mathbf{m} + a \begin{pmatrix} \cos \phi \\ \sin \phi \end{pmatrix} \quad \text{and} \\ \mathbf{o} &= \mathbf{m} + b \begin{pmatrix} \cos(\phi + \alpha) \\ \sin(\phi + \alpha) \end{pmatrix}. \end{aligned}$$

We thus obtain after some simplification

$$\mathbf{g}_2(\mathbf{m}) \cdot \overline{\mathbf{p}\mathbf{o}} = h(a + b)(1 - \cos \alpha),$$

which implies

$$\left(\int \int \mathbf{g}_2(\mathbf{m}) d\xi d\eta \right) \cdot \overline{\mathbf{p}\mathbf{o}} \geq 0.$$

As a result, we have

$$|\mathbf{F}| \geq \left| \int \int \mathbf{g}_1(\mathbf{m}) d\xi d\eta \right| = k|\mathbf{p}\mathbf{o}|A, \quad \text{and}$$

$$\mathbf{F} \cdot \overline{\mathbf{p}\mathbf{o}} = \left(\int \int \mathbf{g}_1(\mathbf{m}) + \mathbf{g}_2(\mathbf{m}) d\xi d\eta \right) \cdot \overline{\mathbf{p}\mathbf{o}} \geq 0. \quad \blacksquare$$

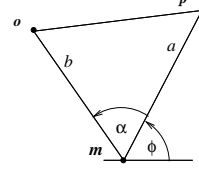


Figure 7: Arrangement of point M with respect to the pivot point and the center.

Proof of Lemma 4

For $h > 0, k = 0$, this is reduced to the case of the unit radial field for which a proof is given in [5, 6]. For $h, k > 0$, let us assume that $P_1 \neq P_2$ are two pivot points of \mathcal{J} . By definition, when P_1 is positioned at the center \mathbf{o} , the part is in an equilibrium. Now let us translate the part such that P_2 is positioned at \mathbf{o} . By Lemma 2, the magnitude of the resultant force induced by \mathcal{J} is $|\mathbf{F}| \geq k|\mathbf{p}_1\mathbf{o}|A > 0$, where \mathbf{p}_1 is the position of P_1 . Therefore the part cannot be in an equilibrium and the assumption is contradicted. The uniqueness of the pivot point is thus guaranteed.

To prove the existence of the pivot point, consider the part at a fixed orientation θ and the lifted potential energy $U_\theta(x, y)$ of the field \mathcal{J} at the fixed orientation as a function of the position $(x, y)^T$ of the part. Since the function U_θ is induced from the potential function $u(\xi, \eta) = h\sqrt{\xi^2 + \eta^2} + \frac{k}{2}(\xi^2 + \eta^2)$, it is obvious that as the position (x, y) diverges, $U_\theta(x, y)$ increases toward infinity. Because U_θ is continuous, this implies that there exists a critical point where $F_x = \frac{\partial U_\theta}{\partial x} = 0$ and $F_y = \frac{\partial U_\theta}{\partial y} = 0$. This also implies an equilibrium because zero force results in zero moment for every radial field (the line of action of the resultant force induced by a radial field always passes through the center of the field). ■

Note that the proof of Lemma 2 only relies on the definition of the pivot point, not on the uniqueness property, therefore the reference to Lemma 2 in the proof of Lemma 4 does not create an invalid reasoning loop.

References

- [1] S. Akella, W. Huang, K. Lynch, and M. Mason. Sensorless parts orienting with a one-joint manipulator. In *IEEE Int. Conf. on Robotics and Automation (ICRA)*, pages 2383–2390, Albuquerque, NM, April 1997.
- [2] D. Berkowitz and J. Canny. Designing parts feeders using dynamic simulation. In *Proc. IEEE Int. Conf. Robotics and Automation*, Minneapolis, MN, 1996.
- [3] D. Biegelsen, W. Jackson, A. Berlin, and P. Cheung. Air jet arrays for precision positional control of flexible media. In *Proc. Int. Conf. on Micromechatronics for Information*

- and Precision Equipment, pages 631–634, Tokyo, Japan, 1997.
- [4] K.-F. Böhringer, B. Donald, and N. MacDonald. Upper and lower bounds for programmable vector fields with applications to MEMS and vibratory plate parts feeders. In Jean-Paul Laumond and Mark Overmars, editors, *Algorithms for Robotic Motion and Manipulation*, pages 255–276. A. K. Peters, Ltd, Wellesley, MA 02181, 1997.
- [5] K.-F. Böhringer, B. R. Donald, R. Mihailovich, and N. C. MacDonald. Sensorless manipulation using massively parallel microfabricated actuator arrays. In *IEEE Int. Conf. on Robotics and Automation*, pages 826–833, 1994. San Diego, CA.
- [6] K.-F. Böhringer, B. R. Donald, L. Kavraki, and F. Lamiraux. Part orientation with one or two stable equilibria using programmable vector fields. *IEEE Transactions on Robotics and Automation*, 16(2), 2000, pages 157-170.
- [7] K.-F. Böhringer, V. Bhatt, and K.Y. Goldberg. Sensorless manipulation using transverse vibrations of a plate. In *Proc. IEEE Int. Conf. on Rob. and Autom.*, pages 1989–1996, 1995.
- [8] G. Boothroyd, C. Poli, and L. Murch. *Automatic Assembly*. Marcel Dekker, Inc., 1982.
- [9] Y.B. Chen and D.J. Ierardi. The complexity of oblivious plans for orienting and distinguishing polygonal parts. *Algorithmica*, 14:367–397, 1995.
- [10] M. Erdmann and M. Mason. An exploration of sensorless manipulation. *IEEE Tr. on Rob. and Autom.*, 4(4):369–379, 1988.
- [11] F. Lamiraux and L. Kavraki. Positioning and Orienting Symmetric and Non-Symmetric Parts Using a Combination of a Unit Radial and Constant Force Fields. *International Workshop on the Algorithmic Foundation of Robotics*, TH28-TH42, March, 2000.
- [12] K. Y. Goldberg. Orienting polygonal parts without sensors. *Algorithmica*, 10:201–225, 1993.
- [13] M. Jakiela and J. Krishnasamy. Computer simulation of vibratory parts feeding and assembly. In *Proc. 2nd Int. Conf. Discrete Element Methods*, 1993.
- [14] L. E. Kavraki. Part orientation with programmable vector fields: Two stable equilibria for most parts. In *Proc. IEEE Int. Conf. on Robotics and Automation*, pages 2446–2451, 1997.
- [15] O.D. Kellogg. *Foundations of Potential Theory*. Dover, New York, 1953.
- [16] J. Luntz, W. Messner, and H. Choset. Velocity field design for parcel manipulation on the virtual vehicle, a discrete distributed actuator array. In P.K. Agarwal, L. E. Kavraki, and M. Mason, editors, *Robotics: The Algorithmic Perspective*, pages 35–47. AK Peters, Natick, MA, 1998.
- [17] Barrett O’Neill. *Elementary Differential Geometry*. Academic Press, San Diego, 1966.
- [18] Ahmed A. Shabana. *Computational Dynamics*. John Wiley & Sons, New York, 1994.
- [19] A. Sudsang and L. Kavraki. *A force field for orienting and positioning parts in the plane*. Technical Report, Department of Computer Science, Rice University, In preparation.